

Fig. 2 (A) UV-vis-NIR absorption spectra of **1**, **2** and **1 + 2** as recorded in trichloromethane at 298 K. (B) Partial ¹H NMR spectra (600 MHz, 298 K) of (a) **2** (0.7 mM), (b) **1** (0.7 mM), (c) **1 + 2** (0.7 mM of **1** and **2**, respectively) and (d) **1 + 2** (7.0 mM of **1** and **2**, respectively) all in trichloromethane-d₁. (C) 2D NOESY NMR spectroscopy of **1** (7 mM) and **2** (7 mM) in trichloromethane-d₁.

for this conclusion came from UV-vis-NIR and NMR spectroscopic studies involving **2**. Specifically, a new CT band at 566 nm is seen in the UV-vis-NIR spectrum of **1 + 2** recorded in trichloromethane that is not present in the spectrum of the individual components (Fig. 2A). In addition, upfield shifts in the signals ascribed to the nitrophenyl aryl protons and downfield shifts are seen for the pyrrole NH signals in the ¹H NMR spectrum recorded of a mixture of **1 + 2** (CDCl₃) as compared to the individual components. These effects become more pronounced at higher concentrations (Fig. 2B). They are also seen when **2** is replaced by either **3** or **4**. In addition, 2D ¹H NOESY NMR studies reveal clear cross peaks between protons on **1** and **2** (Fig. 2C).

Diffraction grade single crystals from all three combinations of **1** and **2–4**, corresponding to (1·2)_n, (1·3)_n and (1·4)_n, were obtained (Fig. 3A–C; see ESI† for crystallographic tables). The corresponding X-ray diffraction structures revealed that extended supramolecular aggregates are stabilised in the solid state. Based on the structural parameters, these polymeric structures are thought to be stabilised through a combination of donor acceptor and hydrogen bond interactions involving the pyrrolic NHs of **1** and the nitro groups present in **2–4**. However, the specific structures differ from one another. For instance, while the structures of (1·2)_n and (1·3)_n both consist of monomeric subunits arranged in a head-to-tail fashion, their monomeric subunits arranged in a linear fashion, *gauche* interactions are present in the linking subunit of (1·3)_n that are not present in (1·2)_n. Even more dramatic differences are seen in the case of (1·4)_n; here, the individual subunits are arranged in a T-like manner (Fig. 3).

An effort was made to correlate the X-ray single crystal structures with the extent of association observed in solution. Towards this end, absorption changes produced at 490 nm were monitored as a function of concentration when **1** is mixed with **2**, **3** or **4** in trichloromethane. The observed changes could be fit well to a 1:1 binding profile in all cases. This allowed *K*_a values of 1.5 (± 0.3) × 10³, 1.3 (± 0.3) × 10³, and 3.8 (± 0.6) × 10³ L mol⁻¹ to be calculated

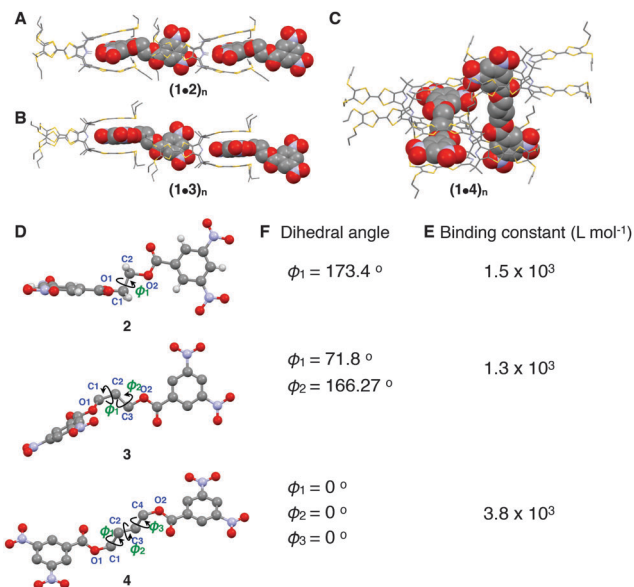


Fig. 3 (A–C) X-ray single crystal structures of (1·2)_n, (1·3)_n and (1·4)_n. (D and E) Dihedral angles for the linkers present in monomers **2–4** as deduced from the solid state structural parameters. (F) Binding constants calculated from UV-vis-NIR spectroscopic titrations carried out in trichloromethane.

for (1·2)_n, (1·3)_n and (1·4)_n, respectively.⁸ The observed variations in binding affinities are ascribed to differences in steric hindrance between the monomeric constituents, which are relatively reduced in (1·4)_n and (1·2)_n in comparison to (1·3)_n, as inferred from the individual structures in question and from inspection of the dihedral angles for the spacers linking the electron deficient subunits in **2–4** (cf. Fig. 3D and E).

Support for the notion that the individual subunit–subunit interactions are highest in the case of (1·4)_n, as compared to (1·2)_n and (1·3)_n, came from 2D diffusion ordered (DOSY) NMR spectroscopic studies (see ESI† Fig. S14). For instance, in the case of similar equimolar mixtures in CDCl₃, the lowest diffusion coefficient was seen in the case of **1** and **4**, as would be expected for systems that undergo a higher relative degree of self-association.

Of the three self-assembled systems considered in this study, namely (1·2)_n, (1·3)_n and (1·4)_n, the best solubility was observed in the case of (1·2)_n. This ensemble was thus used to examine the effect of solvent. Towards this end, two solvents, namely 1,2-dichloroethane (DCE) and methylcyclohexane (MCH), with greater and lower polarity, respectively, than trichloromethane, were used. Based on variable temperature UV-vis-NIR spectroscopic studies, an inverse relationship between the calculated binding constants (Table 1) and the solvent polarity was observed. The effect was notable, with the use of MCH providing an increase in the *K*_a value by more than two orders of magnitude relative to what is seen in trichloromethane (Table 1).

Continuous-variation (Job) plots for **1** and **2** provided further support for the contention that the *K*_a value is higher in MCH than in trichloromethane (Fig. 4A). For instance, in MCH, the mole fraction at which the concentration of the complex was maximal was 0.5, as would be expected for an association that was 1:1 (or 2:2, or 3:3, etc.). However, a slight deviation was

Table 1 Thermodynamic properties of the supramolecular aggregates, $(\mathbf{1}\cdot\mathbf{2})_n$, formed from the ditopic donors and acceptors **1** and **2** as deduced from temperature-dependent absorption spectroscopic analyses carried out in 1,2-dichloroethane (DCE) and methylcyclohexane (MCH). The values listed assume an isodesmic model

Solvent	Concentration [mM]	ΔH [kJ mol ⁻¹]	T_m [K]	K_e^a [L mol ⁻¹]	ΔS [J mol ⁻¹ K ⁻¹]	DPN ^a
CHCl ₃	1.6	NA	NA	$1.5 (\pm 0.3) \times 10^3$	NA	1.7
1,2-Dichloroethane	0.4	-28.1	265.0	$3.9 (\pm 0.3) \times 10^2$	-72	1.0
Methylcyclohexane	0.1	-106	330.8	$4.8 (\pm 0.1) \times 10^5$	-249	16

^a Values determined at 293 K.

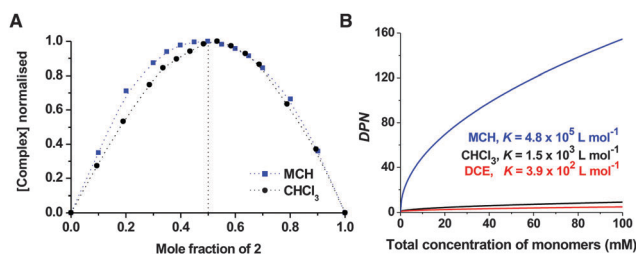


Fig. 4 (A) Continuous variation plots for the solution phase interaction between **1** and **2** as observed in methylcyclohexane and trichloromethane, respectively. (B) Plots of DPN as a function of monomer concentration in different solvents, based on the binding constants in Table 1.

seen in trichloromethane, notwithstanding the reasonable fit to a 1 : 1 binding profile that was observed under conditions of the UV-vis binding titrations (*vide supra*).

This deviation is ascribed to the presence of a small quantity of (TTF-C4P : bis-dinitrophenyl) complex with net 2 : 1 stoichiometry (Fig. 4A). Such deviations from pure 1 : 1 stoichiometry are expected in the case of weaker net K_a values.

To analyze the effect of solvent polarity on the degree of polymerisation (DPN), the DPN was plotted as a function of concentration in MCH, DCE, and trichloromethane. In the case of trichloromethane and DCE, the degree of polymerisation is extremely low and does not show a meaningful increase as the total concentration of monomers goes up. On the other hand, in MCH strong concentration-dependent behaviour was seen with the DPN increasing with concentration. This is consistent with what is expected for a system characterised by a relatively higher binding constant.

In summary, mixing the TTF functionalised ditopic C[4]P receptor **1** with any of the three congeneric bis-dinitrophenyl functionalised acceptors **2–4** leads to formation of supramolecular self-assembled ensembles. Fully polymeric structures are seen in the solid state in the case of all three acceptors.

In trichloromethane solution, the interactions are weak and are seen to vary with the choice of linker. The highest intra-component interactions are seen in the case of **4**, followed by **2**, an observation ascribed to steric effects. The effect of structure is rather large, with an order of magnitude difference in the K_a

value being observed when comparing **1-3** and **1-4** (Fig. 3) in trichloromethane. The effect of solvent is even greater, as inferred from studies of **1-2** in trichloromethane, DCE and MCH. In the case of the latter solvent, a 1 : 1 binding stoichiometry was inferred from curve fits of the binding profile based on UV-vis-NIR spectroscopic titrations and from Job plots. The derived equilibrium constant for the individual interactions, $K_a = 4.8 \times 10^5$ L mol⁻¹, translates to an effective DPN, of 16 at 0.1 mM in MCH assuming an isodesmic model. In contrast, very little polymerisation is observed in trichloromethane, even at 1.6 mM. The present results, which highlight the effect of external parameters on the self-assembly of weakly associated systems, may serve to increase our understanding of the factors that influence aggregation in a way that might not be possible using systems that self-associate with high binding affinity.

This work was supported by the National Science Foundation (grant CHE-1057904 to J.L.S.), the Robert A. Welch Foundation (grant F-1018 to J.L.S.), the Villum Foundation (to J.O.J.), and the Danish Natural Science Research Council (FNU, Project 11-106744 to J.O.J.).

Notes and references

- C. Schmuck and W. Wienand, *Angew. Chem., Int. Ed.*, 2001, **40**, 4363–4369.
- M.-O. M. Piepenbrock, G. O. Lloyd, N. Clarke and J. W. Steed, *Chem. Rev.*, 2010, **110**, 1960–2004.
- B. Zheng, F. Wang, S. Dong and F. Huang, *Chem. Soc. Rev.*, 2012, **41**, 1621.
- R. P. Sijbesma, F. H. Beijer, L. Brunsveld, B. J. Folmer, J. H. Hirschberg, R. F. Lange, J. K. Lowe and E. W. Meijer, *Science*, 1997, **278**, 1601–1604.
- Y. Li, T. Park, J. K. Quansah and S. C. Zimmerman, *J. Am. Chem. Soc.*, 2011, **133**, 17118–17121.
- X. Yan, B. Jiang, T. R. Cook, Y. Zhang, J. Li, Y. Yu, F. Huang, H.-B. Yang and P. J. Stang, *J. Am. Chem. Soc.*, 2013, **135**, 16813–16816.
- N. N. Adarsh and P. Dastidar, *Chem. Soc. Rev.*, 2012, **41**, 3039–3060.
- J. S. Park, K. Y. Yoon, D. S. Kim, V. M. Lynch, C. W. Bielawski, K. P. Johnston and J. L. Sessler, *Proc. Natl. Acad. Sci. U. S. A.*, 2011, **108**, 20913–20917.
- D. S. Kim, V. M. Lynch, J. S. Park and J. L. Sessler, *J. Am. Chem. Soc.*, 2013, **135**, 14889–14894.
- K. A. Nielsen, W. S. Cho, J. O. Jeppesen, V. M. Lynch, J. Becher and J. L. Sessler, *J. Am. Chem. Soc.*, 2004, **126**, 16296–16297.